

Supporting information

Mn²⁺ activated Ca- α -SiAlON – Broadband deep-red luminescence and sensitization by Eu²⁺, Yb²⁺ and Ce³⁺

Atul D. Sontakke,^a Arnoldus J. van Bunningen,^a Sadakazu Wakui,^{a,b} and Andries Meijerink^a

^a *Condensed Matter & Interfaces, Debye Institute for Nanomaterials Science, Utrecht University, Princetonplein 1, 3584 CC Utrecht, The Netherlands*

^b *Nichia Corporation, 491 Oka, Kaminaka-Cho, Anan-Shi, Tokushima 774-8601, Japan*

Contents:

Figure S1: Normalized PL emission spectra of Mn²⁺ (10 at.%) doped Ca- α -SiAlON samples obtained using fluoride and oxide doping precursors.

Figure S2: PLE spectra of Mn²⁺ (10 at.%) doped Ca- α -SiAlON samples obtained using fluoride and oxide doping precursors.

Figure S3: PXRD patterns of Ca- α -SiAlON samples doped with 0 – 15 at.% Mn²⁺ contents.

Figure S4: PLE spectra of Mn²⁺ (1 – 15 at.%) doped Ca- α -SiAlON in semi-log scale. The charge transfer band (< 350 nm) exhibits maximum intensity for 5 at.% Mn²⁺ contents, whereas the d-d transition bands (> 350 nm) exhibits maximum for 10 at.% Mn²⁺.

Figure S5: Mn²⁺ PL decay curve in 1 at.% doped Ca- α -SiAlON and respective multi-exponential fit. The curve exhibits good fit with three exponential fitting. The slowest component exhibits decay lifetime of 2.1 ms.

Figure S6: Mn²⁺ PL-PLE spectra at 4.2 K. The zero phonon line (ZPL) is weak and is estimated to be at around 593 nm. The PL-PLE crossing point also occurs at around 593 nm.

Figure S7: Temperature dependent PL spectra of Mn²⁺ (10 at.%) doped Ca- α -SiAlON under 443 nm excitation.

Figure S8: Schematic configuration crossover model suggesting lower activation energy (E_a) for red-shifted emission transitions.

Figure S9: 4.2 K PLE spectra of Mn²⁺ (10 at.%) doped Ca- α -SiAlON monitoring at different emission regions. The PLE feature reveals prominent variation at 428 nm and 443 nm with respect to monitoring wavelength.

Figure S10: Figure S10: 4.2 K vibronic fine-structure of Mn²⁺ orange-red PL observed in Ba s-phase and AlN (top). PXRD pattern of Ba s-phase and reference patterns (bottom).

Figure S11: Figure S11: PL-PLE spectra of Eu²⁺ singly doped and Eu²⁺-Mn²⁺ codoped Ba s-phase compounds (top). Eu²⁺ PL decay curves in singly and codoped samples (bottom).

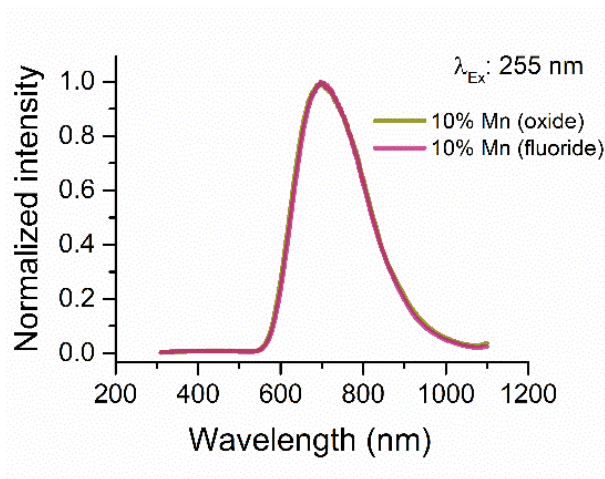


Figure S1: Normalized PL emission spectra of Mn²⁺ (10 at.%) doped Ca- α -SiAlON samples obtained using fluoride and oxide doping precursors.

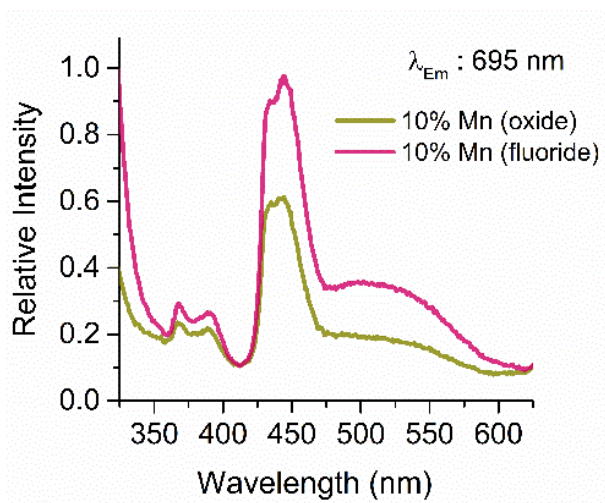


Figure S2: PLE spectra of Mn²⁺ (10 at.%) doped Ca- α -SiAlON samples obtained using fluoride and oxide doping precursors.

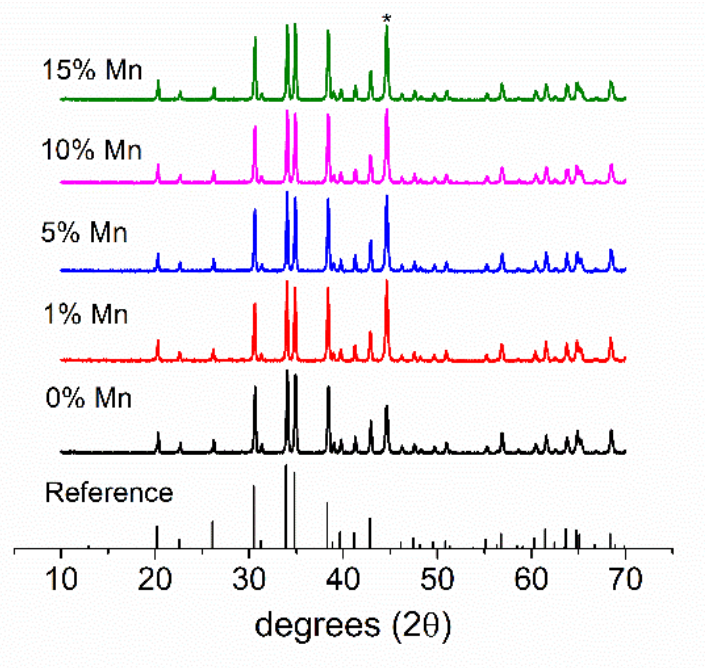


Figure S3: PXRD patterns of Ca- α -SiAlON samples doped with 0 – 15 at.% Mn²⁺ contents. All sample holder reflections appear at about 39^o, 45^o and 65^o.

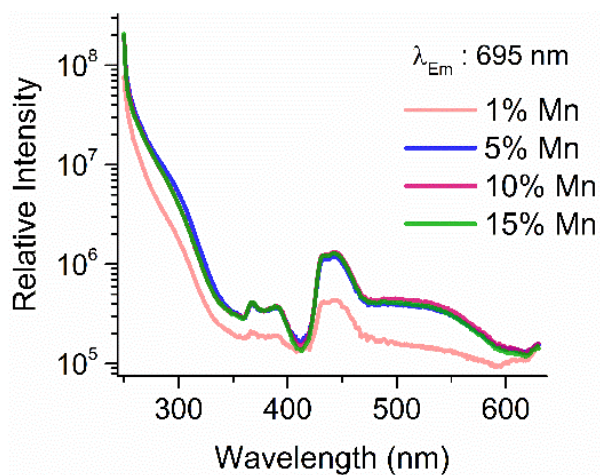


Figure S4: PLE spectra of Mn²⁺ (1 – 15 at.%) doped Ca- α -SiAlON in semi-log scale. The charge transfer band (< 350 nm) exhibits maximum intensity for 5 at.% Mn²⁺ contents, whereas the d-d transition bands (> 350 nm) exhibits maximum for 10 at.% Mn²⁺.

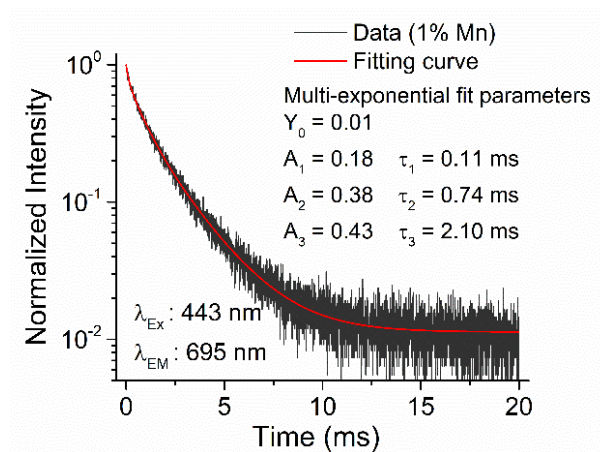


Figure S5: Mn^{2+} PL decay curve in 1 at.% doped Ca- α -SiAlON and respective multi-exponential fit. The curve exhibits good fit with three exponential fitting. The slowest component exhibits decay lifetime of 2.1 ms.

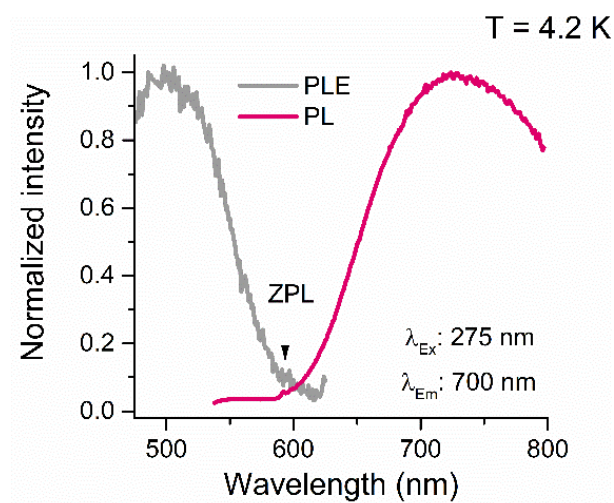


Figure S6: Mn^{2+} PL-PLE spectra at 4.2 K. The zero phonon line (ZPL) is weak and is estimated to be at around 593 nm. The PL-PLE crossing point also occurs at around 593 nm.

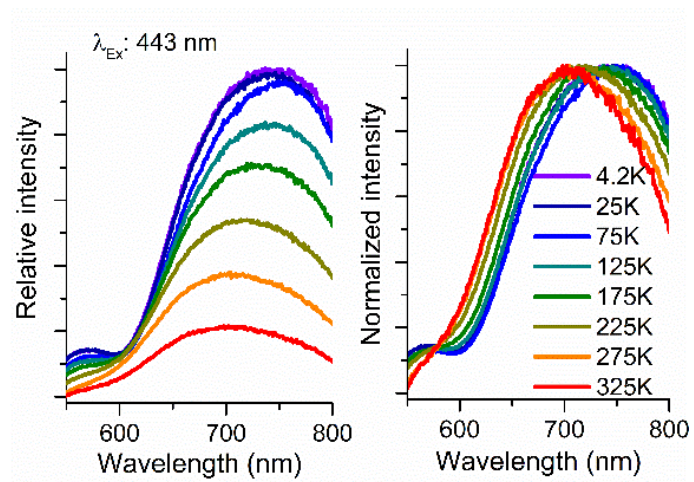


Figure S7: Temperature dependent PL spectra of Mn^{2+} (10 at.%) doped $\text{Ca-}\alpha\text{-SiAlON}$ under 443 nm excitation.

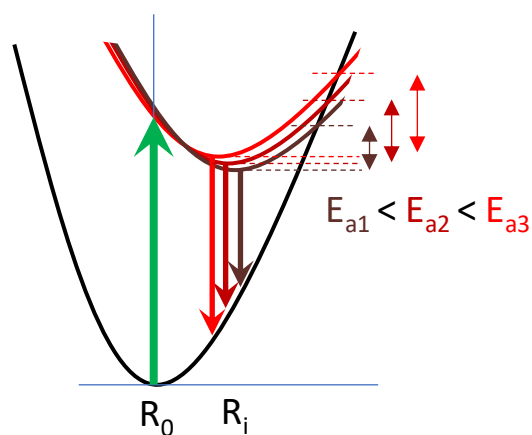


Figure S8: Schematic configuration crossover model suggesting lower activation energy (E_a) for red-shifted emission transitions.

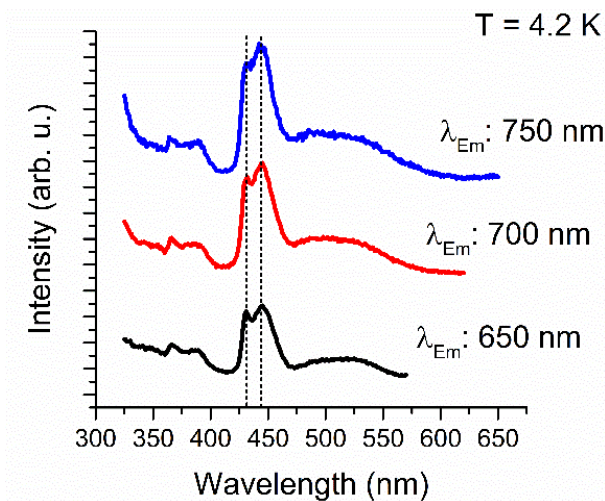


Figure S9: 4.2 K PLE spectra of Mn^{2+} (10 at.%) doped Ca- α -SiAlON monitoring at different emission regions. The PLE feature reveals prominent variation at 428 nm and 443 nm with respect to monitoring wavelength.

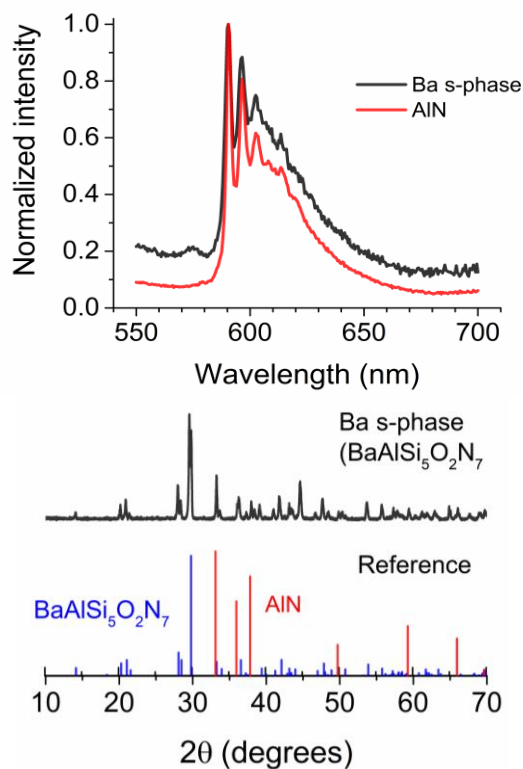


Figure S10: 4.2 K vibronic fine-structure of Mn^{2+} orange-red PL observed in Ba s-phase and AlN (top). PXR pattern of Ba s-phase and reference patterns (bottom). Al sample holder reflections appear at about 39° , 45° and 65° .

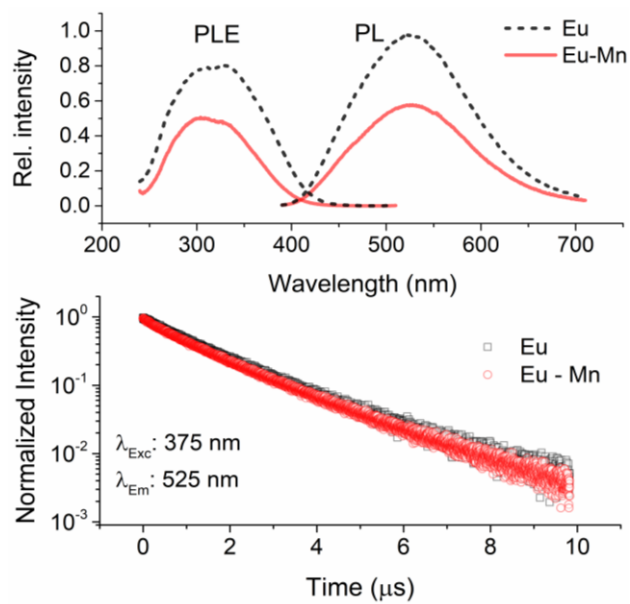


Figure S11: PL-PL spectra of Eu^{2+} singly doped and $\text{Eu}^{2+}\text{-Mn}^{2+}$ codoped Ba s-phase compounds (top). Eu^{2+} PL decay curves in singly and codoped samples (bottom). The dopant concentration is 5 at% for Eu^{2+} as well as Mn^{2+} .